KF post deposition treatment in N_2 of single-stage thin $Cu(In,Ga)Se_2$ absorber layers

Jessica de Wild[a, b, c], Thierry Kohl[a, b, c], Dilara G. Buldu[a, b, c], Gizem Birant[a, b, c], David Mate Parragh[b, e, f], Guy Brammertz[a, b, c], Marc Meuris[a, b, c], Jef Poortmans[c, d, e], Bart Vermang[a, b, c]

[a] Institute for Material Research (IMO), Hasselt University, Agoralaan gebouw H, Diepenbeek, 3590, Belgium

[b] Imec division IMOMEC (partner in Solliance), Wetenschapspark 1, Diepenbeek, 3590, Belgium.

[c] Energyville, Thor Park 8320, Genk, 3600, Belgium

[d] imec (partner in Solliance), Kapeldreef 75, Leuven, 3001, Belgium

[e] Department of Electrical Engineering, KU Leuven, Kasteelpark Arenberg 10, Heverlee, 3001, Belgium

[f] Department of Combustion Technology and Thermal Energy, University of Miskolc, 3515 Miskolc-Egyetemváros, Hungary

***Abstract* — Thin (<500 nm) single-stage co-evaporated Cu(In, Ga)Se_2 (CIGS) absorber layers are treated with a KF post anneal in N_2 atmosphere. The conditions of the post anneal, initial acceptor concentration and the temperature are varied. Solar cells are characterized with current-voltage and capacitance-voltage measurements. Efficiencies up to 12% with an open circuit voltage (V_{oc}) of > 640 mV were achieved after KF treatment. From SCAPS simulations and IVT measurements it is concluded that the V_{oc} of these cells are limited by back-contact surface recombination and thus further improvements require passivation of the back contact.**

***Index terms* — Cu(In, Ga)Se_2, alkali treatment, thin absorber, single-stage process**

I. Introduction

Thin film $Cu(In,Ga)Se_2$ (CIGS) solar cells have reached an efficiency beyond 23%. However, when going to modules the efficiency is max 19% but often less [1]. One reason for this large gap is that the process steps that are required to make the individual solar cells so efficient are not easily upscalable for module production. One way to resolve this, is to make the CIGS solar cells structure simpler and more cost effective. We are aiming to achieve this by decreasing the thickness to ~ 500 nm and using an ungraded absorber layer grown with a single stage co-evaporation step. This makes the process simpler, fast and requires less material. However, since the thin layers are rather different in their compositional depth profile and grain size compared to the thicker 3-stage co-evaporated layers, re-investigation of some commonly used process steps like alkali addition is required. In this contribution we investigate the effect of the KF post deposition treatment (KF-PDT) in N_2 atmosphere on our thin ungraded absorber layers. K has been shown to deplete the surface and grain boundaries from copper [2], [3] [4], which results in a surface band gap widening [5], [6]. This surface band gap widening improves the pn junction properties [2] and reduces recombination at the grain boundaries and thus improves the quality of the absorber layer [7].

To investigate the effect of KF-PDT, we use a Mo/Si(O,N)/soda lime glass substrate. The Si(O,N) layer functions as an alkali diffusion barrier and in this way the amount of alkali can be controlled. Initial results were published in [8], and revealed improvements due to KF-PDT up to 2% absolute. In this contribution the temperature and method of the anneal are varied as well as the initial acceptor concentration N_A by changing the initial amount of NaF. We found that the open circuit voltage (V_{oc}) can be further improved until it becomes limited by back contact recombination. Efficiencies up to 12% are achieved with the new anneal method.

II. Experimental details

Absorber layers were grown with a single-stage co-evaporation process at a substrate temperature of 550 °C. K was added by spin coating a 0.2M KF solution onto the absorber layers. Details can be found in [8]. The Na was added by evaporating NaF on the Mo prior to CIGS absorber layer growth. The samples were annealed further in a tube oven in a N_2 atmosphere at 300 or 400 °C for 20 minutes. The CIGS surface was either covered or exposed to the N_2 flow, see figure 1. As cover the SLG/Si(O,N)/Mo substrate was used and placed on top

of the absorber layer with the Mo side down. Covering the absorber layer possibly reduces Se escape from the absorber and may even create a local Se atmosphere. Having the Mo side down, avoids direct contact with the soda lime glass that could interfere with the alkali. When the cover is applied, the samples will be referred to as 'covered' and when the sample had no cover it will be referred to as 'exposed'. After the KF-PDT the samples were without any rinsing or etching covered with CdS by chemical bath deposition. The different samples that are prepared can be found in table 1. The composition and the thickness of all samples were determined with XRF. The thickness of the absorber layers is 480 ± 40 nm, the Cu/(In + Ga) ratio 0.85 ± 0.5 and the Ga/(In + Ga) ratio 0.31 ± 0.2. Absorber layers were finished into solar cells with sputtered i-ZnO-AZO window layers and evaporated Ni/Al/Ni grids as front contact. The cells were mechanically scribed and have an area of 0.5 mm^2. Solar cells were characterized with (temperature dependent) current voltage (JV(T)), capacitance voltage (CV) and external quantum efficiency (EQE) measurements. From the dark JV curves, the series and shunt resistances were determined as well as J_0 for samples coming from the same co-evaporation run.

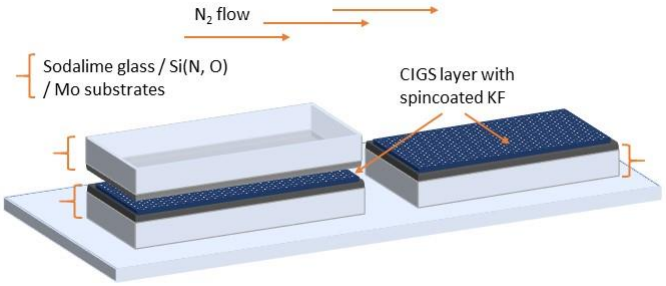

Fig.1. Post deposition annealing methods: CIGS layer covered with the substrate (left) or exposed to the nitrogen flow (right).

TABLE I

SAMPLE MATRIX OF THE DIFFERENT KF-PDTS

Sample number	NaF supply (evaporation)	KF supply (M)	Anneal temperature (°C)
1	2 nm	-	300, exposed
2	2 nm	0.2	300, exposed
3	2 nm	-	400, exposed
4	2 nm	0.2	400, exposed
5	7 nm	-	400, exposed
6	7 nm	0.2	400, exposed
7	2 nm	0.2	400, covered

III. RESULTS

A. *Solar Cells*

Solar cells were made of the different KF treated absorber layers, summarized in table 1. The baseline has 2 nm NaF and no K. Finished solar cells were characterized with JV and CV measurements. We find increased device performance, for all KF treatments, attributed to increased V_{oc} and FF. Results are presented in figure 2 and the values of the best cell from each run are summarized in table II. The V_{oc}s of the exposed cells are about 560-580 mV after the KF treatment, and neither annealing temperature nor initial NaF amount result in significant differences in V_{oc}. The covered sample has a V_{oc} of 640 mV, corresponding to an increase of about 100 mV. The FF increases about 2% absolute for the exposed samples, without any significant differences for temperature and initial NaF amount, to 7% for the covered sample. This increase in FF cannot be attributed to changes in shunt and series resistances. The FF is mainly affected by changes in the space charge region [9], while the V_{oc} is heavily affected by interface defects. Hence, these results imply that without covering mainly the bulk is improved, while with covering the front surface is also affected causing an improved pn junction and higher V_{oc}. Finally, we determined the J_0s for the samples annealed at 400 ºC from the measured dark curves. The results are presented in figure 2 on the right. Here we found an approximately one order decrease of the J_0 for the KF treated cells. There were no major differences in J_0 found between the covered and the exposed samples, though the V_{oc} of the covered sample is significantly higher. A more detailed study on the effect of covering of the absorber layer during the post anneal can be found elsewhere [10].

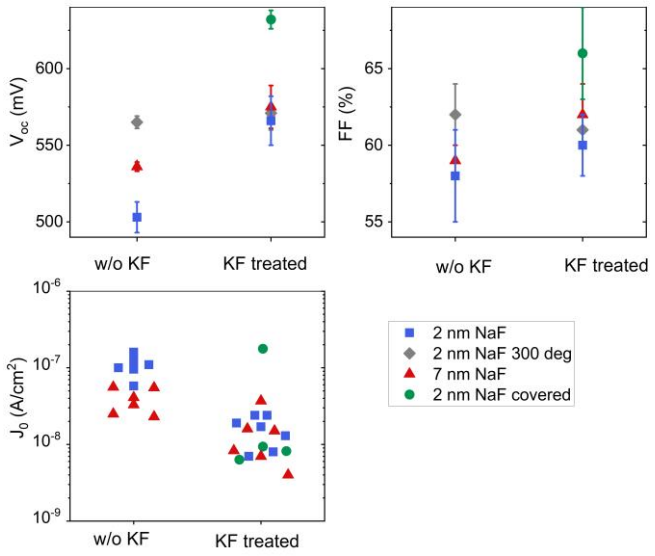

Fig. 2. JV (V_{oc}, FF nd J_0) parameters of thin single-stage KF treated and untreated CIGS solar cells for the various NaF amounts and annealing conditions given in table 1. The J_0 values are extracted from the dark curves.

TABLE II

JV-PARAMETERS FOR THE BEST CELLS. THE SAMPLE NUMBER CORRESPONDS TO THE DIFFERENT ALKALI TREATMENTS PRESENTED IN TABLE I.

Sample number	V_{oc} (mV)	J_{sc} (mA/cm^2)	FF (%)	J_0 (A/cm^2)	η (%)
1	567	18.7	61.7	-	6.6
2	582	20.0	61.7	-	7.2
3	540	26.0	59.5	$2.3\cdot10^{-8}$	8.4
4	586	24.0	62.6	$4.0\cdot10^{-9}$	8.8
5	515	19.3	59.3	$5.8\cdot10^{-8}$	5.9
6	581	24.8	62.3	$7.0\cdot10^{-9}$	9.0
7	640	29.5	64.9	$6.4\cdot10^{-9}$	12.3

We showed in a previous contribution that the apparent acceptor concentration N_A increases after KF treatment. However, different V_{oc}s were observed for similar doping profiles after the KF treatment, related to the presence or absence of Na in the absorber layer prior to the KF treatment [8]. In the literature both decrease [11] as well as increase [12], [13] in the net acceptor concentration have been reported upon KF treatment while the V_{oc} improved in all cases. Whether the acceptor concentration increases or decreases upon KF treatment might depend on the initial acceptor concentration due to copper vacancies and its equilibrium with the alkali [14]. Here we increased the N_A by adding more NaF (7 nm instead of 2 nm) and performed KF treatment under exposed atmosphere. We determined the doping for the reference and the KF treated cells. The results are presented in Figure 3. For the sample with 2 nm NaF we observe an increase in N_A with the KF-PDT as observed before. For the sample with 7 nm NaF however, we have a higher N_A without KF than with KF treatment. Via the relationship:

$$\Delta V_{oc} = \frac{k_B T}{q} ln \frac{N_{A_{KF}}}{N_{A_{w/oKF}}}$$

we can calculate an expected increase/decrease in V_{oc} due to the changes in doping. We used the lowest values of N_A determined from the CV measurements to calculate the expected change in V_{oc} due to doping changes. The values are presented in table 3. A decrease of about 10 mV and an increase of 16 mV were calculated due to the net acceptor decrease/increase. However, we do observe a V_{oc} increase in both cases, resulting in similar V_{oc}s after KF treatment for the exposed samples. Hence, the change in doping upon KF treatment has a marginal impact on the change in V_{oc}.

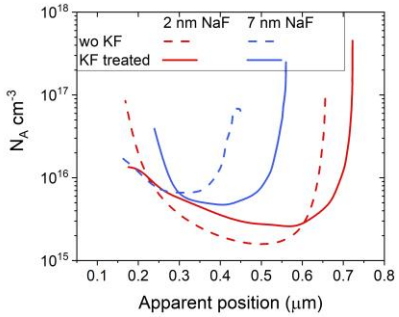

Fig. 3. Doping profile determined from capacitance voltage measurements. Change of acceptor concentration with KF treatment: decrease if the acceptor concentration is very high (blue lines), increase if the acceptor concentration is low (red lines).

TABLE III

EXTRACTED N_A AND CALCULATED V_{oc} CHANGE

NaF amount (nm)	N_A untreated (10^{15} cm^{-3})	N_A treated (10^{15} cm^{-3})	ΔV_{oc} (mV)
2 nm	1.5	2.7	+16
7 nm	6.6	4.6	- 10

IVT measurements were performed on the cell with the highest V_{oc} and a reference cell. The band gap was determined from EQE measurements, to be compared with the extrapolated V_{oc} value at 0 K. The results are presented in figure 4. The band gaps of both cells are about 1.24 eV. The extrapolated V_{oc} at 0 K for both cells are 1.15 eV, which is slightly lower than the band gap. This likely means that an interface is limiting the solar cells performance [15]. The front interfaces are different of both cells due to the KF treatment, making it unlikely that the front interface is limiting the efficiency and more likely that the back-contact limits the V_{oc}.

SCAPS simulations are used to investigate the effect of the net acceptor concentration N_A and thickness using a high back recombination velocity of 10^6 cm/s on the V_{oc}. This value is expected for the CIGS/Mo interface if there is no passivation layer [16]. The results are presented in figure 5. We find that the effect of N_A on the V_{oc} is marginal and a maximum V_{oc} of about 640 mV for a 500 nm thick absorber layer can be achieved. This is what we measured as well. We observe that up to 700 nm, the thickness has a very strong effect on the $V_{oc,}$ indicating that back recombination is limiting the V_{oc} for thicknesses less than 700 nm. Hence, to improve the V_{oc} of the 500 nm thin absorber layer further, passivation of the back contact is required. Passivation of the Mo back contact is under investigation and improvements are reported by several groups, and recently a review is published on the progress that is made on back contact passivation in thin CIGS solar cells [17].

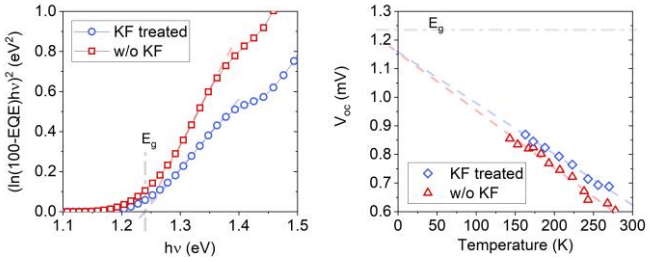

Fig. 4. Left: EQE measurements to extract the band gaps of both cells (w/o KF and covered KF treated). Right: IVT measurements to extract the V_{oc}s at 0 K for the same cells as those for the EQE. The band gaps are 1.24 eV and the V_{oc}s at 0 K are 1.15 eV. This is slightly lower than the band gap, indicating an interface is limiting the efficiency for both cells.

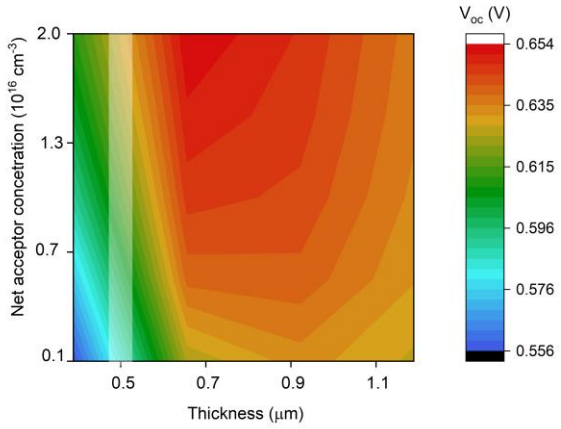

Fig. 5. SCAPS simulation with changing doping and thickness. The white shaded area is the thickness of the absorber layer used in the experiments. The input parameters are from [18]. The V_{oc} is highly dependent on the thickness, and to a lesser extent on the net acceptor concentration.

IV. Conclusions

KF-PDT was performed on single-stage thin absorber layers in N_2 atmosphere. We find improvements for all KF treated cells, with the highest V_{oc} achieved for the covered sample. We also found that the net acceptor concentration can either decrease or increase upon the KF treatment depending on the initial acceptor concentration. The temperature of the PDT step did not affect the final V_{oc}, efficiency or FF as they were similar for both 300 and 400 ºC. Neither did the initial amount of NaF result in significantly different V_{oc}s or FF. With SCAPS simulations and from IVT measurements we conclude that the covered KF treated cells are limited by recombination at the back contact. Higher efficiencies for the single stage processed absorber layers may then be achieved by applying KF treatment on back-passivated absorber layers. The overall efficiency has increased almost 4% compared to the baseline (that is 2 nm NaF) reaching over 12% efficiency for our 500 nm single stage processed solar cells. It shows the potential of the simplified methodology to reach highly efficient thin CIGS solar cells.

Acknowledgments

This work received funding from the European Union's H2020 research and innovation program under grant agreement No. 715027

References

[1] M. A. Green, E. D. Dunlop, D. H. Levi, J. Hohl-Ebinger, M. Yoshita, and A. W. Y. Ho-Baillie, "Solar cell efficiency tables (version 54)," *Prog. Photovoltaics Res. Appl.*, vol. 27, no. 7, pp. 565–575, Jul. 2019.

[2] J. A. Aguiar *et al.*, "Revealing Surface Modifications of Potassium-Fluoride-Treated Cu(In,Ga)Se $_2$: A Study of Material Structure, Chemistry, and Photovoltaic Performance," *Adv. Mater. Interfaces*, vol. 3, no. 17, p. 1600013, Sep. 2016.

[3] A. Chirilă *et al.*, "Potassium-induced surface modification of Cu(In,Ga)Se2 thin films for high-efficiency solar cells," *Nat. Mater.*, vol. 12, no. 12, pp. 1107–1111, Dec. 2013.

[4] N. Nicoara, T. Lepetit, L. Arzel, S. Harel, N. Barreau, and S. Sadewasser, "Effect of the KF post-deposition treatment on grain boundary properties in Cu(In, Ga)Se2 thin films," *Sci. Rep.*, vol. 7, p. 41361, Jan. 2017.

[5] E. Handick *et al.*, "Potassium Postdeposition Treatment-Induced Band Gap Widening at Cu(In,Ga)Se $_2$ Surfaces – Reason for Performance Leap?," *ACS Appl. Mater. Interfaces*, vol. 7, no. 49, pp. 27414–27420, Dec. 2015.

[6] P. Pistor *et al.*, "Experimental indication for band gap widening of chalcopyrite solar cell absorbers after potassium fluoride treatment," *Appl. Phys. Lett.*, vol. 105, no. 6, p.

063901, Aug. 2014.
[7] N. Nicoara *et al.*, "Direct evidence for grain boundary passivation in Cu(In,Ga)Se2 solar cells through alkali-fluoride post-deposition treatments," *Nat. Commun.*, vol. 10, no. 1, p. 3980, Dec. 2019.
[8] J. de Wild *et al.*, "Alkali treatment for single-stage co-evaporated thin CuIn0.7Ga0.3Se2 solar cells," *Thin Solid Films*, vol. 671, pp. 44–48, Feb. 2019.
[9] G. Agostinelli *et al.*, "Presented at the 3 rd WCPEC."
[10] J. de Wild *et al.*, "High V_{oc} upon KF Post-Deposition Treatment for Ultrathin Single-Stage Coevaporated Cu(In, Ga)Se_2 Solar Cells," *ACS Appl. Energy Mater.*, vol. 2, no. 8, pp. 6102–6111, Aug. 2019.
[11] F. Pianezzi *et al.*, "Unveiling the effects of post-deposition treatment with different alkaline elements on the electronic properties of CIGS thin film solar cells," *Phys. Chem. Chem. Phys.*, vol. 16, no. 19, p. 8843, Apr. 2014.
[12] A. Laemmle, R. Wuerz, and M. Powalla, "Investigation of the effect of potassium on Cu(In,Ga)Se 2 layers and solar cells," *Thin Solid Films*, vol. 582, pp. 27–30, May 2015.
[13] A. Laemmle, R. Wuerz, and M. Powalla, "Efficiency enhancement of Cu(In,Ga)Se_2 thin-film solar cells by a post-deposition treatment with potassium fluoride," *Phys. status solidi - Rapid Res. Lett.*, vol. 7, no. 9, pp. 631–634, Sep. 2013.
[14] Z.-K. Yuan *et al.*, "Na-Diffusion Enhanced p-type Conductivity in Cu(In,Ga)Se_2: A New Mechanism for Efficient Doping in Semiconductors," *Adv. Energy Mater.*, vol. 6, no. 24, p. 1601191, Dec. 2016.
[15] S. S. Hegedus and W. N. Shafarman, "Thin-film solar cells: device measurements and analysis," *Prog. Photovoltaics Res. Appl.*, vol. 12, no. 23, pp. 155–176, Mar. 2004.
[16] B. Vermang *et al.*, "Introduction of Si PERC Rear Contacting Design to Boost Efficiency of Cu(In,Ga)Se_2" *IEEE J. Photovoltaics*, vol. 4, no. 6, pp. 1644–1649, Nov. 2014.
[17] G. Birant, J. de Wild, M. Meuris, J. Poortmans, and B. Vermang, "Dielectric-Based Rear Surface Passivation Approaches for Cu(In,Ga)Se2 Solar Cells—A Review," *Appl. Sci.*, vol. 9, no. 4, p. 677, Feb. 2019.
[18] C. Frisk *et al.*, "Optimizing Ga-profiles for highly efficient Cu(In, Ga)Se_2 thin film solar cells in simple and complex defect models," *J. Phys. D. Appl. Phys.*, vol. 47, no. 48, p. 485104, Dec. 2014.